Proceeding Paper

Immobilization of Fungal Peroxidase on Paramagnetic Nanoparticles for Synthetic Dye Decolorization [†]

**Kingsley O. Omeje [1],*, Magbo Chinonso [1], Emmanuel C. Ossai [1], Juliet N. Ozioko [1], Benjamin O. Ezema [1],
Nonso E. Nnolim [2] and Sabinus O. O. Eze [1]**

[1] Department of Biochemistry, University of Nigeria, Nsukka, Enugu State, Nigeria,
kingsley.omeje@unn.edu.ng(K.O.O.), ezema.onyebuchi@unn.edu.ng(B.O.E.), juliet.ozi-oko@unn.edu.ng(J.N.O.), emmanuel.ossai@unn.edu.ng(E.C.O.), sabinus.eze@unn.edu.ng(S.O.O.E.)

[2] Applied and Environmental Microbiology Research Group (AEMREG), Department of Biochemistry and Microbiology, University of Fort Hare, Eastern Cape, South Africa; nnolim@ufh.ac.za

* Correspondence: kingsley.omeje@unn.edu.ng;.

[†] Presented at the 3rd International Online Conference on Nanomaterials, Online. 25 April – 10 May, 2022.

Abstract: Peroxidase was produced by *Aspergillus flavus* KIGC on 11th day of fermentation when grown on banana peel as the sole carbon source. It was purified to 8.86 folds with percentage recovery of 49.72%. The purified peroxidase was immobilized on magnetic nanoparticle and characterized using DLS, DSC, XRD, FTIR and SEM analyses. The results suggest adequate nanoparticle formulation and effective enzyme immobilization. Optimal temperatures for free and immobilized peroxidase were 75 and 70 °C, respectively, optimum pH of 5.0 and 9.0 were obtained for free enzyme and 6.5 and 9.0 for immobilized peroxidase, respectively. The Km of 0.075mM and catalytic efficiency of 90.66 Mol/S-1 were achieved by the immobilized peroxidase on guaiacol as substrate. The immobilized peroxidase exhibited enhanced synthetic dyes decolorization ability.

Keywords: Oxidoreductase; dye decolorization; peroxidase; immobilization; bioremediation

1. Introduction

The high cost of commercial peroxidase and high rate of its denaturation as a result of unstable conditions of temperature, pH and organic solvents are some of the major challenges facing industrialists and other users. Furthermore, decreases in enzyme activity, inability to recover and reuse the enzyme are some problems encountered during industrial uses of enzymes. However, to proffer solutions to these problems, enzyme immobilization on some supports aids in overcoming these challenges [1]. The most common materials used in enzyme immobilization include silica, chitosan, clay and polystyrene [1, 2]. Currently, enzyme immobilization on nanoparticles is receiving attention from researchers [3, 4, 5], due to the attendant advantages it confers on enzymes such as improvement in thermal and mechanical property [6]. Also, enzyme activity and stability improve after immobilization [7]. Immobilization of enzymes also exerts addition operational properties such as recovery and reusability to the enzyme [8].

One of the most commonly used industrial enzymes is peroxidase [9], an oxidoreductase responsible the oxidation of broad range of organic compounds. It has several applications in areas such as dye decolorization [10], production of biofuel cells [11], organic synthesis [12], bioremediation of phenolic compounds [13]. Other areas of peroxidase applications include agriculture and environmental sectors [1]. Despite these enormous applications, the cost of peroxidase is high and not always available, thus the need for the production of peroxidase from fungi, a cheap and readily available and cost effective source.

Good rate of growth in agro-waste residue and ability to secrete extracellular enzymes at high concentration are some of the essential features that make fungi good sources of enzymes [14]. Fungi are good sources of enzymes [15]. Thus, this study was designed to evaluate the production and immobilization of peroxidase on metallic nanoparticle from fungal strain cultured using submerged fermentation medium fortified with various agro-wastes as sole carbon source and its ability to decolorize synthetic dyes.

2. Materials and methods

2.1. Materials

2.1.1. Collection of Soil Sample

Soil sample was collected in a sterile bag from an identified area in Nsukka, Enugu State (6°51'24"N 7°23'45"E), Nigeria. Serial dilutions of the samples were prepared up to 10^{-5}. An aliquot was spread on potatoes dextrose agar (PDA) plates and incubated for 7 days for the fungal growth. The isolates obtained were morphologically and taxonomically examined [16]. Isolated fungal strains were maintained on fortified PDA slants and used as stock cultures for the preparation of fresh inoculum for the subsequent experimentations.

2.2. Methods

2.2.1. Peroxidase Production

The production of peroxidase was carried out using submerged fermentation in 250 mL flasks containing 100 mL of basal salt medium (BSM) made of peptone (0.3%), KH_2PO_4 (0.06%), $ZnSO_4$ (0.0001%), K_2HPO_4 (0.04%), $FeSO_4$ (0.0005%), $MnSO_4$ (0.05%) and $MgSO_4$ (0.05%); and glucose (1%) all in w/v. Prior to inoculation, the media were sterilized by autoclaving and the pH was aseptically adjusted to 6.50; subsequently inoculated with nine day old fungal culture (four loops of mycelium $\varnothing$ 3 mm), and incubated at 30°C with shaking for nine days. Thereafter, the media were homogenized using an electric homogenizer and the homogenate separated using a centrifuge (Rotina 380 R Benchtop, Tuttlingen, Germany) at 6000 rpm for 60 min at 4 °C. The supernatant was filtered through a four layer calico cloth and used for the subsequent analysis.

2.2.2. Optimization of fungal medium for peroxidase production

The conditions for peroxidase production by the organism was studied and optimized using different standard carbon sources (sucrose, xylose, glucose, mannose, lactose, arabinose and soluble starch) on the fermentation medium at varying concentrations of 0.1–1.0 g/100 mL. The concentration of the best carbon source was varied from 0.5 to 10.0g/100mL at intervals of 0.5g. The medium pH was also adjusted from pH 3.5 to pH 11.0 at interval of 0.5 units in order to ascertain the optimal fermentation pH. The optimal incubation temperatures (30–45 °C) were varied at intervals of 5 °C. Also, different agro-wastes such as bambara nut husk, banana peel, orange peel, sugar cane baggase and saw dust served as sole source of carbon in the fermentation medium. After the cultivation, the fermentation broth was homogenized using an electric homogenizer and the homogenate was separated into supernatant and cell debris at 6000 rpm for 60 min at 4 °C using a centrifuge (Rotina 380 R Benchtop, Tuttlingen, Germany). The supernatant was further filtered through a four layer calico cloth and the filtrate was utilized to assay for peroxidase activity.

2.2.3. Time course study for peroxidase production

Day of highest peroxidase activity production by the fungal isolate was evaluated by withdrawal of aliquots from fermentation broth every day for 15 days.

2.2.4. Peroxidase purification and molecular weight determination

The crude enzyme was precipitated out of the solution using ammonium sulphate. About 250 g of ammonium sulphate was added in 800 mL of crude enzyme and allowed to stand for 6 h under continuous shaking. The solution was centrifuged at 6000 rpm for 20 min to recover the pellet, and the supernatant was subsequently brought to 70% saturation, which gave maximum protein precipitation. The pellet recovered from the ammonium sulphate precipitation was re-suspended in sodium phosphate buffer (pH 8.0; 0.1 M). The precipitated enzyme was introduced onto a (40.5 × 1.4 cm) DEAE-cellulose anion exchanger column equilibrated with 0.1 M sodium phosphate buffer (pH 8.0). The sample was eluted with discontinuous NaCl gradient of 0.5, 0.1, 0.15 and 0.2 M concentration of NaCl. The active fractions were subjected to the size exclusion chromatography. The active fractions were fractionated by gel filtration on a sephadex G75 column, previously equilibrated with 0.1 M phosphate buffer (pH 8.0). Fractions were collected at a 5 mL flow rate per 5 min, which was used to determine peroxidase activity and protein concentration.For the determination of the enzyme molecular weight, SDS-PAGE was performed in 12% disc gels, as described by Laemmli [17], and the gels stained with silver staining as described Switzer et al. [18] under standard conditions.

2.2.5. Enzyme activity assay

Peroxidase activity was assayed using the method of Eze [19] by measuring the change in absorbance as it oxidizes the o-dianisidine using UV/Vis Spectrophotometer (6405 Jenway, USA). The assay mixture (3 mL) contained of 100 mM phosphate buffer (2 mL, pH 7.0), the substrate (o-dianisidine, 0.3 mL) and crude enzyme (0.4 mL). The reaction was initiated by the addition of hydrogen peroxide (0.3 mL). The peroxidase activity was monitored by change in absorbance (at 470 nm) due to the oxidation of o-dianisidine.

2.2.6. Phylogenetic analysis of the fungal isolate genome

The isolation of the genomic DNA of the potent fungal isolate was doneas described by Pryce [20]. The amplification of the ITS region carried out under standard conditions using polymerase chain reaction where LS266: 5'-GCATTCCCAAACAACTCGACTC-3' and V9D: 5'-TTAAGTCCCTGCCCTTTGTA-3' were used as the universal oligonucleotides for the reverse and forward primers, respectively [22]. The generated sequence of nucleotide was used to carry out blast search in the NCBI database for retrieval of similar sequences after which, multiple sequence alignment was accomplished using the ClustalW program, followed by the construction of the phylogenetic tree.

2.2.7. Synthesis and functionalization of iron oxide magnetic nanoparticles (IOMNPs)

The synthesis of iron oxide magnetic nano-particles was carried out as described by Ranjbakhsh et al.[21]. Into 500 mL round bottom flask, $FeCl_2 \cdot 4H_2O$ (1.25 g) and $FeCl_3 \cdot 6H_2O$ (3.40 g) were dissolved in de-ionized (100 mL) water at 60 °C. Thereafter, 25% $NH_3 \cdot H_2O$ (6 mL) was added and the reactant mixture vigorously stirred at 250 rpm for 60 mins. The obtained black precipitate was separated from the liquid phase using a magnetic field, and washed thrice with phosphate buffered saline (PBS, 100 mM sodium phosphate, 150 mM NaCl, pH 7.4). In order to functionalize them with –NH_2 groups, IOMNPs (300 mg, dry weight) were incubated with 2% (v/v) 3-aminopropyltriethoxysilane (APTS, 30 mL) at 70 °C with shaking (250 rpm)in a water bath. Glutaraldehyde (2%) was added and stirred for 120 mins at 350 rpm [22]. After 24 h, they were washed thrice with PBS and maintained in the same buffer at 4°C until use. The activated IOMNPs was incubated with peroxidase (30 U/ml) at 4 °C for 24 h with continuous shaking at 300 rpm. The IOMNPs-

peroxidase complex was decanted using a magnet and washed five times with deionized water and stored at 4 °C until further use.

2.2.8. Characterization of IOMNPs

Phase identification of the formulated IOMNP was done by X-ray diffraction studies (XRD, Philips Diffractometer, The Netherlands). The particle size was determined using dynamic light scattering (DLS, Malvern Zeta sizer Nano S, Worcestershire, UK), and morphology was determined by Scanning electron microscopy (SEM, FEI Company, Tokyo, Japan). Functional groups were detected using Fourier transforms infrared spectroscopy (FTIR, Shimadzu, Kyoto, Japan). The thermostability of the nanoparticle was determined using differential scanning calorimetry (DSC, Shimadzu, Kyoto, Japan) at a heating rate of 10 °C from 60–300 °C in a hermetically sealed aluminum pan.

2.2.9. Effect of temperature and pH on free and immobilized peroxidase activities

The effect of temperature on free and immobilized peroxidase activities was determined at different temperatures (30–70°C). Also, the effect of pH on free and immobilized peroxidase activities was carried out at different pH values ranging from 3.5–11.0 using 0.1 M sodium acetate (pH 4.0–5.0), 0.1 M sodium phosphate (pH 6.0–8.0), and 1 M Tris-HCl (pH 9.0). The result was presented as peroxidase residual activity, using the criteria described in Enzyme assay section.

2.2.10. Effect of free and immobilized peroxidase on substrate concentration

The rate of two substrates (guaiacol and pyrogallol) metabolism by peroxidase was carried out at varying concentrations of 0.2–1.2g/10 mL. The kinetic parameters (K_M, Vmax, $Kcat$, Catalytic efficiency) were calculated from the Lineweaver–Burk plot, and their derivative constants.

2.2.11. Effect of organic solvents on peroxidase Activity

The influence of some organic solvents – DMSO, methanol, acetone, chloroform and ethanol on free and immobilized peroxidase activities was evaluated after 60mins incubation of the enzyme with the organic solvents. The residual activity was measured as described in Enzyme assay section.

2.2.12. Synthetic dye decolorization by free and immobilized peroxidase

The ability of free and immobilized peroxidase to decolorize synthetic dyes was evaluated according to the method of Victor et al. [10]. The dyes used were three (3) azo dyes (Azo Yellow 6, Basic Blue 22, and Azo Brilliant black) and two (2) Vat dyes (Vat Blue 5 and Acid Blue 74). The reaction mixture containing 0.05 M acetate buffer (2.7 mL, pH 5.0), dye solution (0.1 mL), H_2O_2 (0.1 mL) and the free and immobilized peroxidase (0.1 mL each) was incubated at 37 °C for 60 mins. Subsequently, the absorbance was read at wavelength 614 nm using JENWAY 6404 UV/VIS spectrophotometer. The percentage decolorization of each dye was calculated by using the following equation:

$$\text{Percentage decolorization (\%)} = \frac{Ai - Af}{Ai} \times 100 \tag{1}$$

where Ai = initial absorbance before incubation, Af= final absorbance after incubation.

3. Results

Physicochemical conditions (carbon sources, nitrogen sources, pH, temperature and rate of agitation) were studied for optimal peroxidase production by *Aspergillus flavus* KIGC (Figure 1). The effect of different fermentation temperatures (35–45°C) was studied to ascertain the optimal fermentation temperature for peroxidase production by *Aspergil-*

lus flavus KIGC. At 35°C, the highest peroxidase activity (229.12 ± 1.46 U/min) was obtained. Above this temperature, peroxidase production decreased in peroxidase activity as shown in Figure 2a. Also, the optimal pH for peroxidase production by the organism was evaluated. The result showed highest fungal peroxidase production at pH 7.50, with maximum activity of 301.73 U/min (Figure 2b). At the alkaline pH, (pH 8.0–11.0) the peroxidase production decreased considerably ranging from 34.11 to 27.04 U/min.
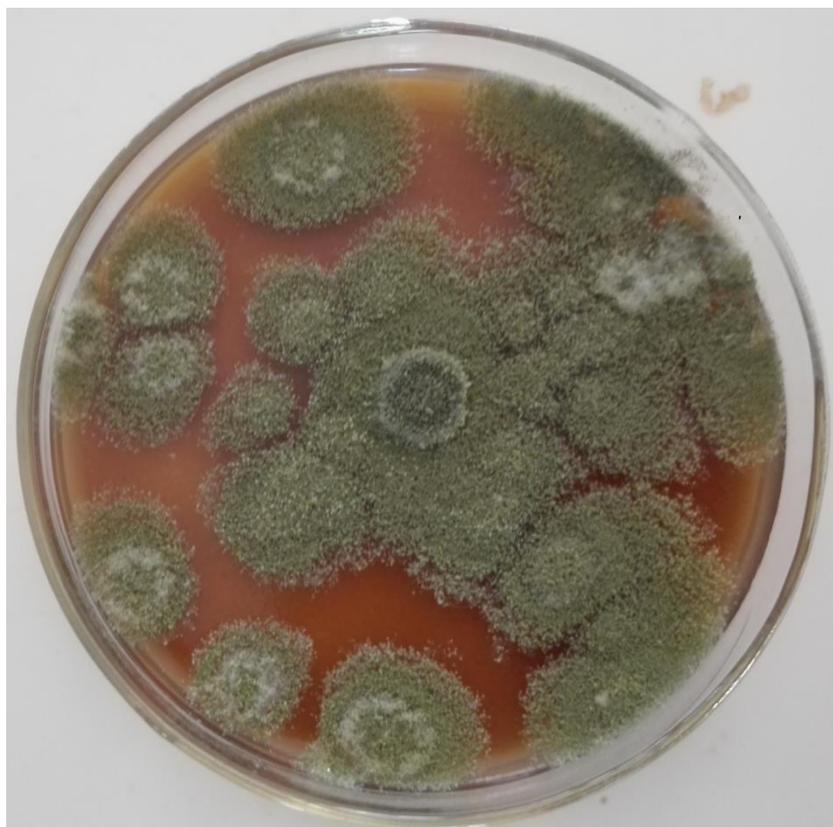

Figure 1. Pure culture of the *Aspergillus flavus* KIGC.
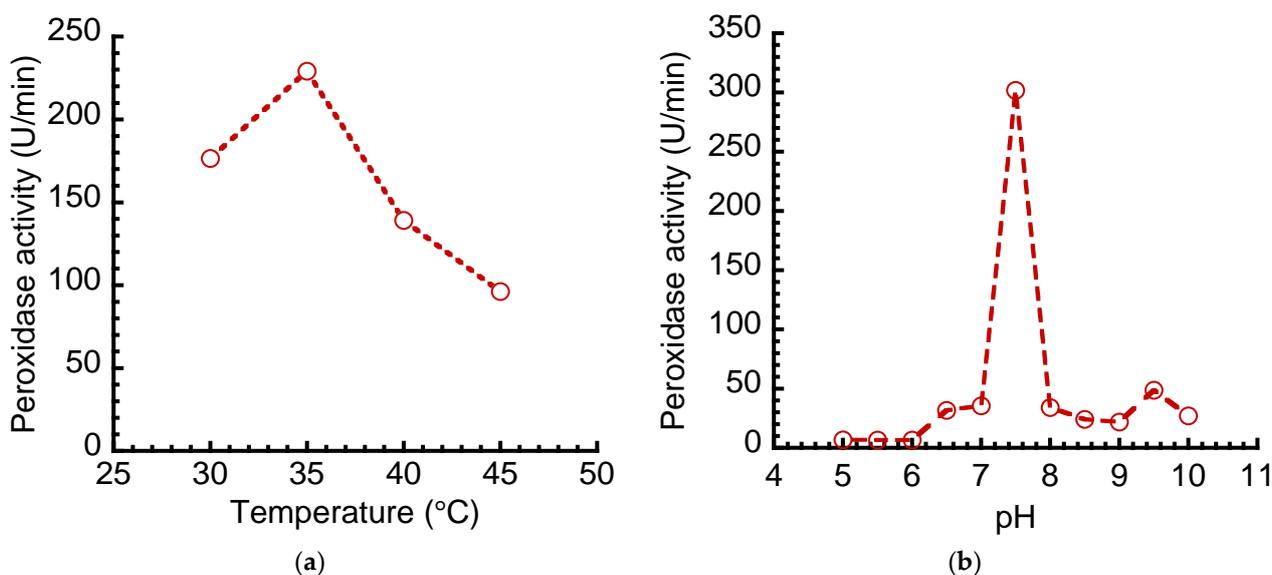
Figure 2. Effects of fermentation (**a**) temperature and (**b**) pH onperoxidase production.

Carbon is an essential nutrient for microbial growth, hence different sources of carbon (sucrose, lactose, mannose, glucose, xylose, arabinose and soluble starch) at varying concentrations (0.1, 0.2, 0.5, 0.8 and 1.0 g/100 mL) were substituted in the fermentation flask for peroxidase production. Peroxidase was produced in the presence of all the carbon sources (sucrose, lactose, mannose, glucose, xylose, arabinose and soluble starch) at different concentrations. Peroxidase activity was highest 296.40 ± 1.54, 440.17 ± 3.18, 483.96 ± 0.87, 276.63 ± 1.21 and 193.26 ± 0.14 U/min in the fermentation media containing glucose at all concentrations 0.1, 0.2, 0.5, 0.8 and 1.0 g/100 mL, respectively when compared to other carbon sources (Figure3a), followed by mannose as the sole carbon source. The least peroxidase activity (12.05 ± 1.24, 39.30 ± 0.76, 22.86 ± 0.11, 37.87 ± 1.42 and 19.36 ± 0.54 U/min) was obtained from the fermentation flask containing soluble starch at all the concentrations studied. Furthermore, the effect of varying glucose concentration on peroxidase activity was evaluated, and 6 g/L was optimal for peroxidase secretion by *Aspergillus flavus* KIGC (Figure 3b). At 10g/L of glucose, there was a drastic reduction in peroxidase activity.
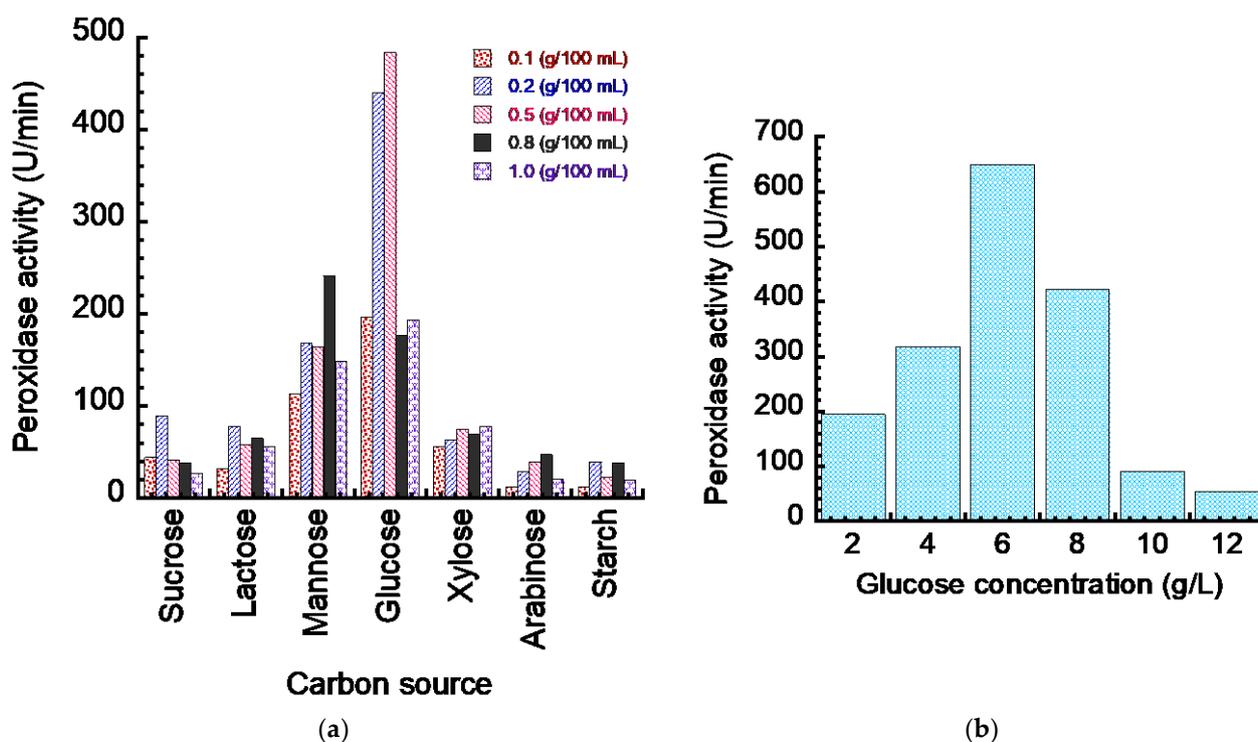

(**a**)　　　　　　　　　　　　　　　　　　　(**b**)

Figure 3. Effects of (**a**) carbon sources and (**b**) glucose concentrations onperoxidase production.

Figure 4 shows the time course study on the production of peroxidase by *Aspergillus flavus* KIGC upon incubation for 15 days. Peroxidase activity was assayed every 24 h, with a progressive increase in peroxidase activity as the days of fermentation increased. On day 11, the highest peroxidase activity (946.17 ± 3.25 U/min) was recorded; above this day, a concomitant decline in the enzyme activity was obtained.
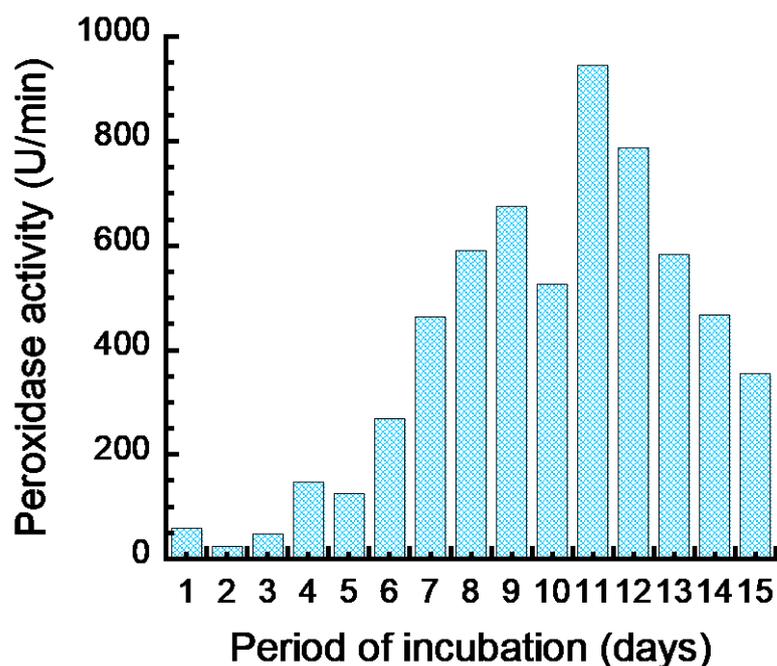
Figure 4. Time course for peroxidase production.

For a cost effective production of peroxidase from *Aspergillus flavus* KIGC, agro-wastes (bambara husk, orange peel, banana peel, sugarcane baggase and sawdust) were used as sources of carbon in the fermentation media. Highest peroxidase production (353.27 ± 0.33U/min) was obtained in fermentation medium containing banana peels as sole carbon source (Figure 5). Fermentation medium with other carbon sources such as orange peels, bambara husk, sugarcane baggase and sawdust had peroxidase activities of 198.39 ± 1.19, 156.87 ± 0.97, 97.02 ± 0.89 and 0.00 U/min, respectively. There was no fungal growth in the fermentation medium containing sawdust.
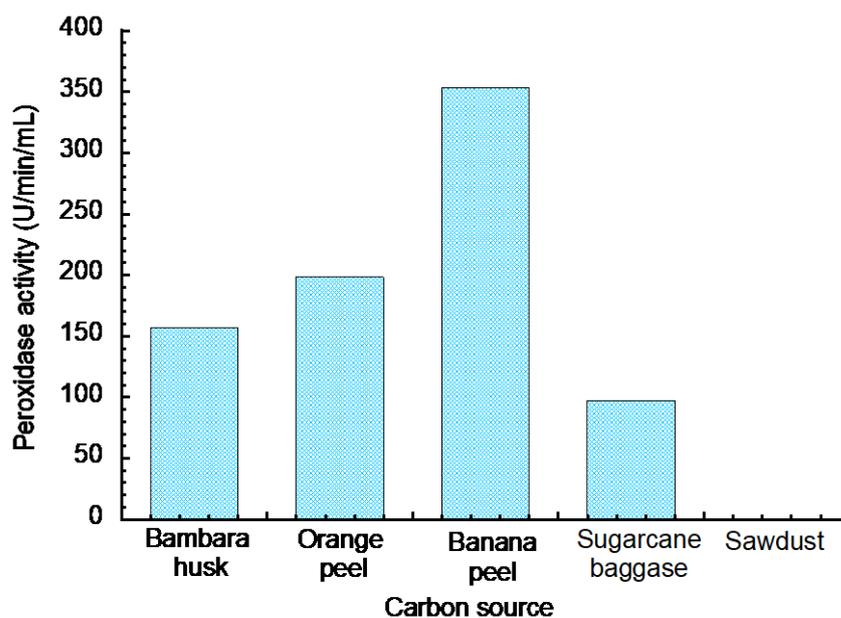

Figure 5. Effects of different agro-wastes as carbon sources on peroxidase production.

Enzyme purification procedures were done using ammonium sulfate precipitation followed by ion exchange chromatography. The last purification process was gel filtration,

giving a final percent yield of 49.72 and purification fold of 8.86 (Table 1).The molecular weight of the purified enzyme was determined using SDS-PAGE, giving a single band of about 57 KDa (Figure 6).
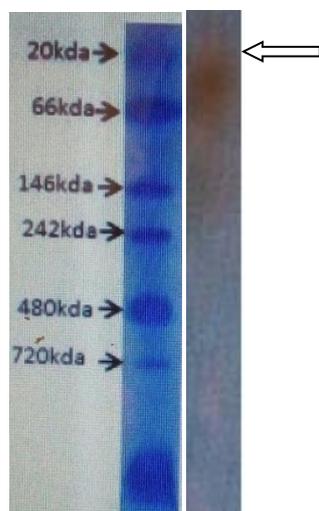

Figure 6. SDS-PAGE analysis of purified peroxidase.

3.1. Identity of the potent fungal isolate

The identification of the potent fungal isolate for peroxidase production gave about 99% sequence similarity with *Aspergillus flavus*TN971D17 (accession number MH329791) based on ITS region sequencing and phylogenetic analysis, and was identified as *Aspergillus flavus* KIGC. The sequence of nucleotide was submitted to the NCBI GenBank with accession number MT951631.The clustering of *A. flavus* KIGC and other related sequences were shown in Figure 7.

The immobilization of peroxidase on metallic nanoparticle was carried out using glutaraldehyde as the cross linker between surface basic amino acids and glutaraldehyde groups on the surface of the particle[25] (Patel et al., 2018). The particle sizes of the free synthesized metallic nano particle and metallic nanoparticle immobilized-peroxidase were 76.20 and 48.01 and 481.20 nm, respectively (Figure 8).The thermostability of the free synthesized metallic and immobilized enzyme was also studied using differential scanning calorimetry (DSC). The DSC thermogram of the formulated nanoparticle showed a melting endothermic peak of 193.97°C (Figure 9). After peroxidase immobilization onto the metallic nano particle, the thermogram showed a melting endothermic peak of 110.92 °C with a broad peak.
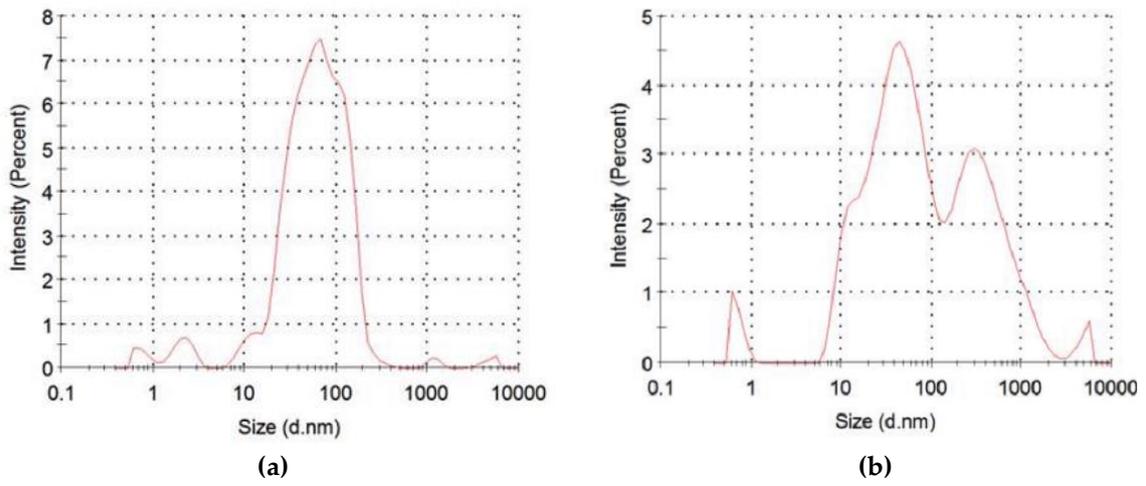
Figure 8. Intensity size distribution of the synthesized iron oxide magnetic nanoparticles and the IOMNP immobilized peroxidase. (a) IOMNP; (b) IOMNP immobilized peroxidase.
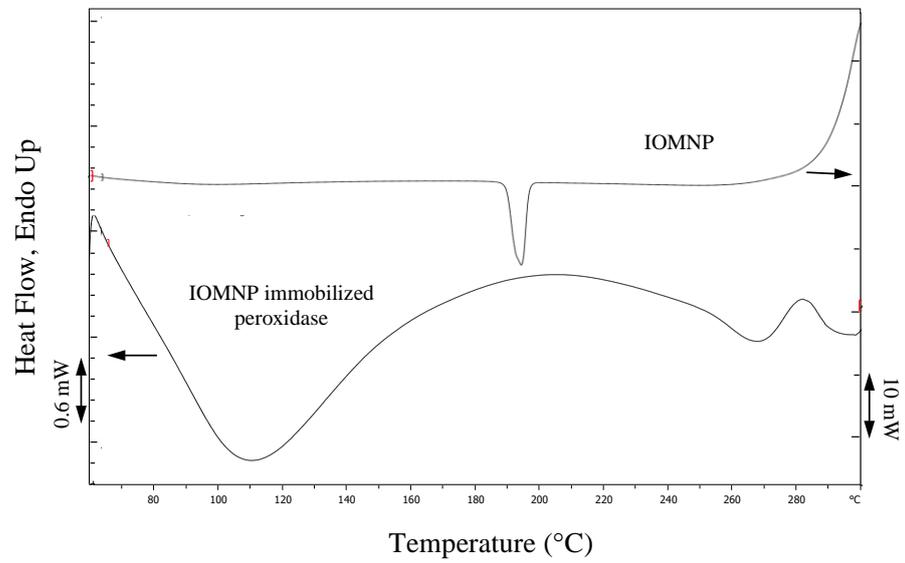

Figure 9. DSC thermogram of the synthesized iron oxide magnetic nanoparticles and the IOMNP immobilized peroxidase.
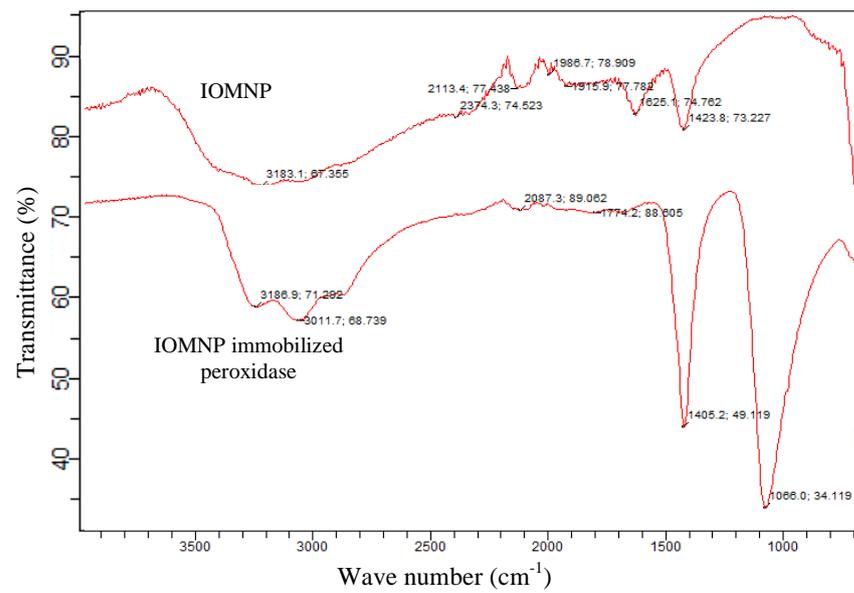
Figure 10. FTIR spectra of the synthesized iron oxide magnetic nanoparticles and the IOMNP immobilized peroxidase.
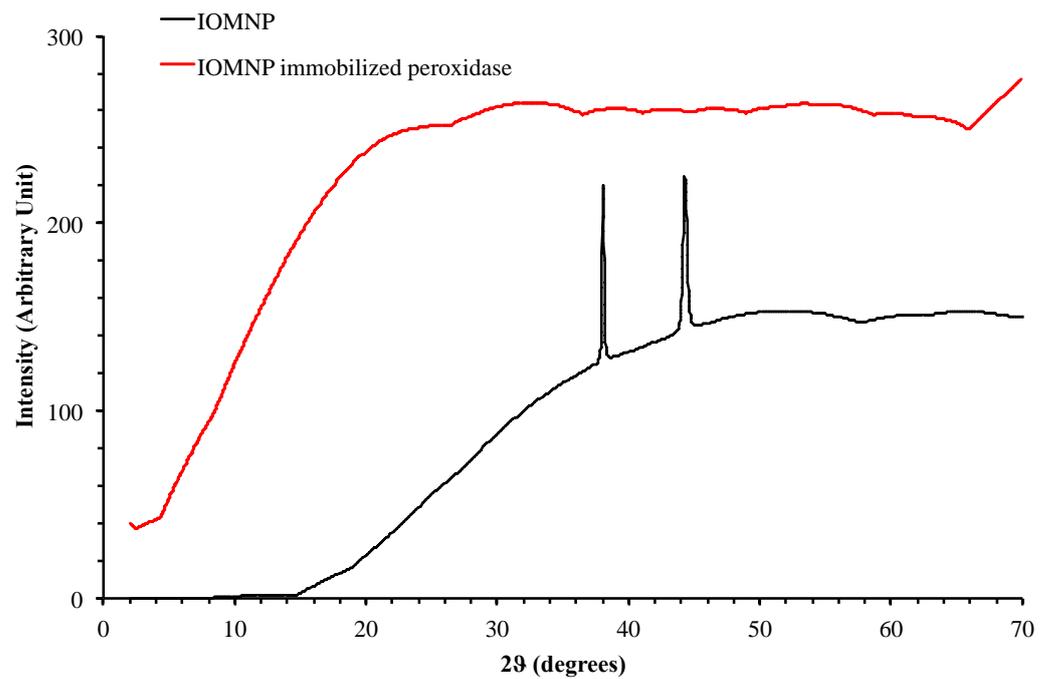

Figure 11. XRD patterns of the synthesized iron oxide magnetic nanoparticles and the IOMNP immobilized peroxidase.

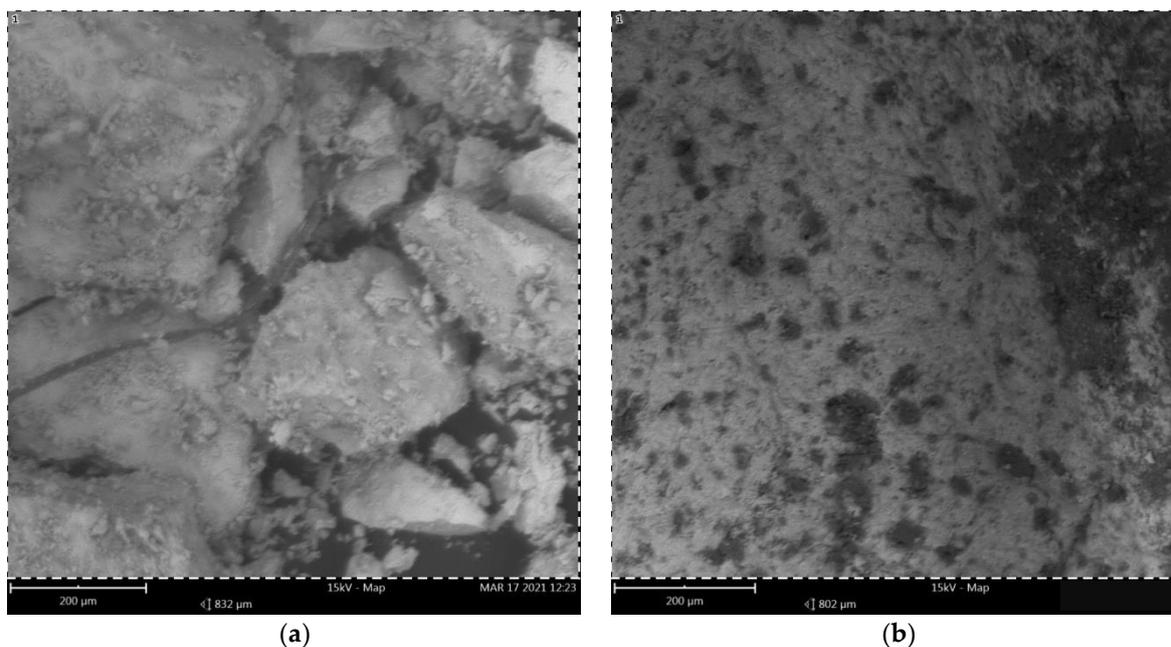(**a**)   (**b**)

Figure 12. SEM images of the synthesized iron oxide magnetic nanoparticles and the IOMNP im-mobilized peroxidase.

Spectra of nanoparticle and nanoparticle-immobilized peroxidase were evaluated us-ing FTIR (Figure 10). Two prominent bands were observed in the synthesized IOMNP at 3000–3400 cm^{-1}and 1625 cm^{-1}.Upon functionalization of the IOMNP with ATPS and sub-sequent anchoring of the enzyme through glutaraldehyde spacer arm, the broad 3000–3400 cm^{-1} transformed into three peaks within the band region.

XRD patterns of free magnetic nanoparticles and magnetic nanoparticle immobi-lized-peroxidase are shown in Figure 11. There was no sharp diffraction peaks in the me-tallic nanoparticle immobilized-peroxidase, unlike the free synthesized metallic nanopar-ticle**.** Also, the morphology of the synthesized nanoparticles and nanoparticle immobi-lized-peroxidase was studied using Scanning Electron Microscopy (Figure 12). Aggre-gates of nanoparticles are seen clustered together with smooth surfaces in the synthesized IOMNP (Figure 12a). After the functionalization of the enzyme through glutaraldehyde spacer arm, the surfaces of the composite became less smooth and indistinct, with greater proportion of open pockets/domains (Figure 12b).

The results of optimal temperature and pH study of free and immobilized peroxidase activity are shown in Figure 13a. The optimal temperatures were 75 and 70 °C, respec-tively, for free and immobilized peroxidase activities. There was successive increase in the enzyme activity as the temperature was increasing until the optimum temperatures, after which a drastic decrease in the enzyme activity was recorded; though, immobilized pe-roxidase had higher activity (826.08 ± 0.32U/min) than the free enzyme (556.61±1.73U/min). Similarly, both free and immobilized peroxidase showed activities at slightly acidic pH region and at pH 9.0, respectively. There was two high peroxidase peaks for the free enzyme at pH 5 (511.30 ± 0.52U/min) and pH 9.0 (443.96 ± 0.34 U/min). At both pH 6.5 and 9.0, peroxidase activities were high for the immobilized enzyme (Figure 13b), as pH tends towards basicity, there was decline in peroxidase activity and the least activ-ity was obtained at pH 9.5.
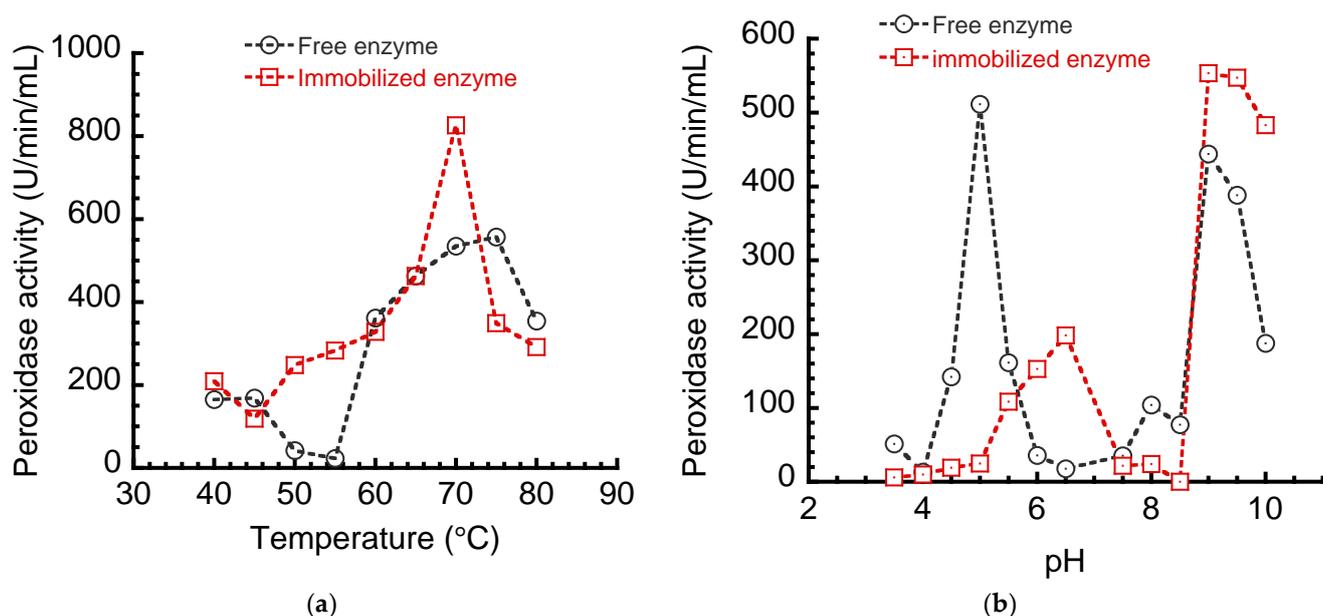
Figure 13. Effects of (**a**) temperature and (**b**) pH on the activity of free and immobilized fungal peroxidase.

To study the kinetic parameters of both free and immobilized peroxidase, varying concentrations of guaiacol and pyrogallol were used at fixed concentration of H_2O_2. The kinetics parameters for free peroxidase (K_M) for guaiacol and pyrogallol were 0.135 and 0.243 mM and V_{max} of 357.14 and 333.33 µmol/min, respectively. Similarly, 0.075 and 1.886 mM were the K_M values obtained for immobilized peroxidase, while 238.09 and 1000 µmoL/min were V_{max} of the immobilized peroxidase, respectively (Table 2). Also, 90.66 and 75.55 moL/S^{-1}were the catalytic efficiencies (turnover rate of guaiacol molecules) of the immobilized and free enzyme, while 39.17 and 15.94 were the catalytic efficiencies for free and immobilized enzyme on pyrogallol as substrate, respectively.

Table 1. Kinetics parameters of free and immobilized peroxidase.

	Free Enzyme		**Immobilized Enzyme**	
	Guaiacol	Pyrogallol	Guaiacol	Pyrogallol
K_m (mM)	0.135	0.243	0.075	1.886
V_{max} (µmoL/min)	357.14	333.33	238.09	1000
$\frac{Vmax}{Km}$	2645.25	1371.74	3174.53	530.22
K_{cat} (min^{-1})	10.204	9.52	6.80	28.57
Catalytic Efficiency(mol/s^{-1})	75.55	39.17	90.66	15.19

The influence of varying concentrations (20, 40, 60 and 80%) of some commonly used organic solvents (DMSO, methanol, acetone, chloroform and ethanol) on free and immobilized peroxidase activity after 60 mins incubation was evaluated. At 20% concentration of all the solvents, more than 80% of peroxidase activity was retained in both free and immobilized peroxidase (Figure 14). For free enzyme, there was a drastic reduction in peroxidase activity as the concentration of DMSO and acetone increased to 80% resulting to residual activities of 44.73 ± 0.69 and 50.11 ± 1.69 U/min, respectively (Figure 14a). More than 70% residual activity of peroxidase was recorded after incubation of the enzyme with methanol and ethanol at all the concentration. Notably, the residual activity of peroxidase increased considerably after incubating the immobilized enzyme for 60 min. at 80%

concentration, more than 60% of peroxidase activity was recovered among all organic solvents except for chloroform that gave 47.72 ± 0.18%. Immobilized peroxidase on iron oxide magnetic nanoparticles exhibited high tolerance when incubated with ethanol > acetone > DMSO > methanol > chloroform, suggesting that ethanol is a better solvent (Figure14b).
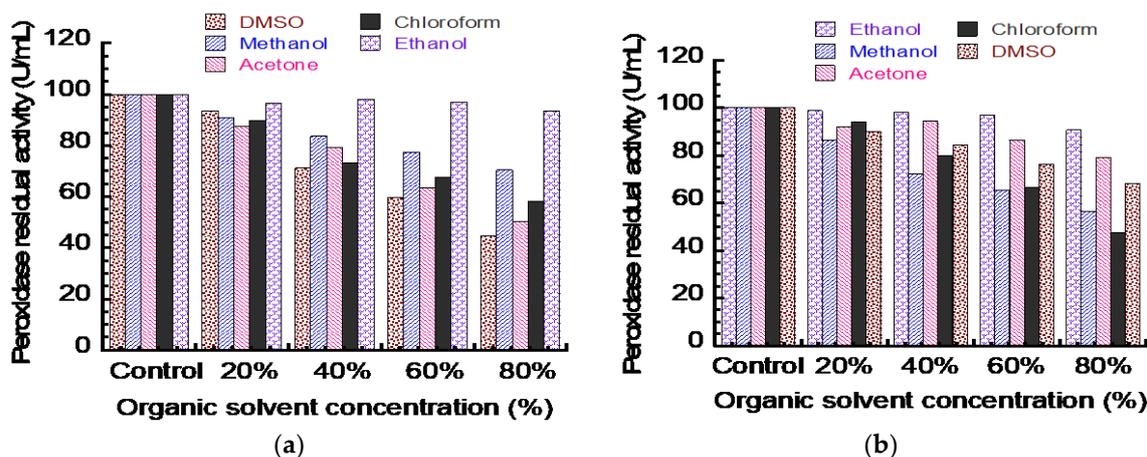

Figure 14. Effect of organic solvents on (a) free and (b) iron oxide magnetic nanoparticle immobilized peroxidase activity.

The ability of free and immobilized peroxidase to decolorize Azo Yellow 6, Basic Blue 22, Azo Brilliant black, Vat Blue 5 and Acid Blue 74 was evaluated after incubation time of 120 min (Figure 15).The free enzyme showed different decolorization rate of textile dyes after 120 min including Azo yellow 6 (76 ± 0.33%), Blue basic 22 (68 ± 2.43%), Azo brilliant Black (55 ± 1.37%), Vat Blue 5 (69 ± 1.35%) and Acid Blue 74 (64 ± 0.75%). On the other hand, immobilized enzyme also exhibited different rate of textile dyes decolorization after 120 min as Azo yellow 6 (89 ± 1.77%), Blue basic 22 (90 ± 0.82%), Azo brilliant Black (71 ± 0.77%), Vat Blue 5 (86 ± 1.60%) and Acid Blue 74 (75 ± 2.08%).
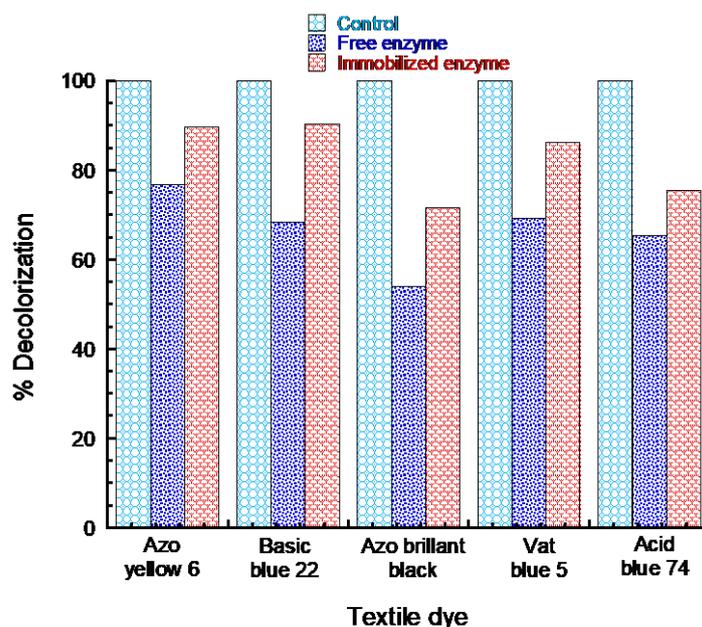

Figure 15. Decolorization potentials of free and immobilized peroxidase on textile dyes.

4. Discussion

Aspergillus species are important sources of enzymes such as laccase [15], pectinase [23], peroxidase [24] and amylases [25]. The extracellular secretion of peroxidase by the isolate was confirmed by the brown coloration of the solid media as a result of guaiacol oxidation. One of the major factors that affect biomolecule production is the constituent of the medium [26]. Thus, cheap and readily available agro-wastes were used as alternative sources of carbon in the fermentation medium. The medium containing banana peel showed high yield of peroxidase, this could be attributed to the presence of some essential nutrients in the peel that encourage microbial growth. The day of highest peroxidase activity was recorded on day 11 of fermentation. Previously, different agro wastes have been reported as good sources of carbon for microbes. Prajapati et al. [24] employed citrus peel in the production of microbial enzyme. Similarly, orange peel and pulp residues were used in enzyme production by some microbial strains [27, 28]. Asgher et al. [29] reported the use of corncob in production of peroxidase by *T. versicolor* on day 5. Also, enzyme production by *P. ostreatus* and *T. hirsuta* was highest on day 9 of fermentation [30, 31]. These differences in day of highest peroxidase activity could be due to variations in the species, source of organism isolation and the nutrient composition of the medium. Day 9 was reported as the day of highest enzyme production by Omeje *et al.* [15].

The final purification fold of the enzyme following sequentially ammonium sulfate, ion exchange, and gel filtration procedures was 8.86 (Table 1). Khatri et al. [32] purified enzyme 1.2 folds from *Aspergillus niger* with specific activity of 8.33 U/min/mg. Also, Dange and Harke [33] purified enzyme from *A. oryzae* up to 67.20%, while 30.65% of activity was reported by Omeje et al. [15] in their work on fungal enzyme. After several steps of enzyme purification (Table 1), molecular mass of 57 KDa was recorded using SDS-PAGE (Figure 6). Researchers have reported similar findings. Molecular mass of 56KDa was reported for *C. cardunculus* peroxidase [34]. The fungal isolate presumably identified as KIGC strain was confirmed as *Aspergillus flavus* due to the similarity of the sequence with other sequences in the NCBI database, and the nucleotide sequence deposited in the GenBank (MT951631). Conventionally, *Aspergillus* spp. have found numerous applications in biotechnological and industrial processesas potential sources for the production of versatile metabolites [35].

The intensity size distribution of the IOMNP gave a modal diameter of 76.20 nm, and upon immobilization of the enzyme, a new peak diameter of 481.20 nm appeared due to the anchoring of the enzyme onto the nanoparticles (Figure 8). The enzyme-immobillized iron oxide metallic nanoparticles showed a broad melting peak temperature 110.92 °C, from 193.97 °C recorded for the bare nanoparticles. The melting temperature of the composite is quite high, and would be suitable for most industrial applications operating below 110 °C. The broadness of the endothermic peak at 110.92 °C couldbe due to water molecules adsorbed unto the surface of the composite material (Figure 9). Two prominent bands observed at 3000–3400 cm^{-1}and 1625 cm^{-1} for the synthesized IOMNP correspond to OH-stretching and OH-bending, respectively, of the metallic NPs. The immobilization of the enzyme onto the IOMNP through ATPS and glutaraldehyde spacer arm transformed the broad 3000–3400 cm^{-1} bands into three peaks, corresponding to vibrations of secondary amines, N-Hof the enzyme's amino groups and those of the APTS, suggesting firm anchoring of the enzyme onto the IOMNPs. Also, peak at 1625 cm^{-1} of the bare IOMNP disappeared upon immobilization of the enzyme onto the NP, resulting to a less prominent peak at 1774 cm^{-1}, due to C=O stretching of glutaraldehyde (Figure 10). Similarly, the disappearance of the diffraction peaks on the free IOMNP upon enzyme immobilization suggests that the formulated enzyme-NP composite material possesses no crystalline phases as a result of the immobilization of the enzyme, unlike the two prominent peaks on the bare IOMNP due to the lattice arrangement of the iron atoms (Figure 11). From the SEM results, the anchoring the enzyme onto the metallic nanoparticles increased considerably the roughness of the surface of the enzyme-NP composite and appearance

of open domains in therein (Figure 12). These observations are indicative of change in morphology and increase in average size of IOMNP upon enzyme immobilization.

Temperature and pH are some important factors that affect enzyme activity. Optimal temperatures for both free and immobilized peroxidase were 75 and 70 °C respectively (Figure 13a). These are high when compared to the temperature optima of 40°C reported by [9]. Also, 45 °C was the optimal temperature of peroxidase extracted from cabbage [10]. Similarly, the optimum pH peaks at 5.0 and 9.0 were obtained for free enzyme while metallic nanoparticle–immobilized peroxidase showed optimum pH of 6.5 and 9.0, respectively. The appearance of two peroxidase activity peaks at both acidic and alkaline pH for both free and immobilized peroxidase could be attributed to the presence of enzyme isoforms, which aids the survival of the enzymes at different pH ranges. [15] reported optimum pH of 7.5 for fungal enzyme. This result is in accordance with the work by [10] who reported optimum pH of 5.0. The pH 5.0 obtained for the free enzyme is in accordance the report by Osuji et al. [36]. The variation in peroxidase activity at the acidic region could be associated with the presence of the immobilized material, which could not interfere with the enzyme activity at the alkaline region (Figure 13b) The kinetic features of the metallic nano-particle immobilized peroxidase on two substrates (guaiacol and pyrogallol), indicated in Table 1, show that the enzyme has high affinity for guaiacol (K_M = 0.075 mM), with catalytic efficiency of 90.66 M^{-1} s^{-1} than pyrogallol (K_M = 1.886 mM) and catalytic efficiency (Turnover rate) of 15.19 M^{-1} s^{-1}. The free enzyme showed more affinity for guaiacol (K_M = 0.135 mM) than pyrogallol (K_M = 0.243 mM), with higher catalytic efficiency of 75.55 M^{-1} s^{-1}. Kinetic paramtere (K_M) of 2.00 mg/mL was reported towards guaiacol [9], while [10] reported Michaelis constant (K_m) of 3.68 Mm on O-dianisidine as substrate. Previous reports have shown that peroxidase has more affinity towards guaiacol than pyrogallol and o-dianisidine [37–39].

Figure 14a shows different residual peroxidase activity after 60 min incubation of the free peroxidase with some common industrial solvents (DMSO, methanol, acetone, chloroform and ethanol). At 80% concentration of ethanol and methanol, more 70% peroxidase residual activity was recovered. The ability of an enzyme to offer resistance to some organic industrial solvents makes it more versatile for industrial uses [1], hence, the ability of the purified fungal peroxidase to retain more than 60% of its activity in these solvents (Figure 14b) suggests it as a good industrial enzyme. Also, peroxidase of soybean hull origin showed highest activity in ethanol, acetone and methanol [40]. Similarly, [1] reported highest peroxidase activity in ethanol and butanol and report by [41] showed 40% in peroxidase activity in the presence of ethanol.

Dye decolorization potential of free and metallic nanoparticle immobilized peroxidase of Azo yellow 6, Basic blue 22, Azo brilliant black, Vat blue 5 and Acid blue 74 were compared with the free enzyme. The metallic nanoparticle immobilized peroxidase showed more decolorization ability on all the dyes studied as compared to that of free enzyme (Figure 15). [10] earlier reported synthetic dye decolorization potential of peroxidase. Also, [15] reported the decolorization of dyes by fungal enzyme. Decolorization of crystal violet using free peroxidase was reported by [42], bromophenol blue [43]. [44] reported high dye decolorization efficiency by immobilized lignin peroxidase.

5. Conclusion

Fungal peroxidase was extracted on the 11th day of submerged fermentation while banana peel served as the sole carbon source, purified and successfully immobilized onto iron oxide magnetic nanoparticle. The immobilized enzyme showed high optimal temperature and active within a broad range of pH and better kinetic results of affinity and catalytic efficiency (Turnover rate) towards guaiacol as substrate. Also, it possesses greater dye decolorization potential than the free enzyme, and was tolerant to some organic solvent, which makes it an important biocatalyst for various industrial applications.

References

1. Pandey, V.P.; Rani, J.; Jaiswal, N.; Singh, S.; Awasthi, M.; Shasany, A.K.; Tiwari, S.; Dwivedi, U.; Chitosan immobilized novel peroxidase from Azadirachta indica: Characterization and application. *Int. J. Biol. Macromol.* **2017**, 104, 1713–1720.
2. Patel, S.K.S.; Choi, S. H.; Kang, Y. C.; Lee, J. K. Eco-friendly composite of Fe$_3$O$_4$-reduced graphene oxide particles for efficient enzyme immobilization. *ACS Appl. Mater. Interfaces* **2017**, 9, 2213–2222
3. Patel, S.K.S.; Otari, S. V.; Li, J.; Kim, D.R.; Kim, S.C.; Cho, B.K.; Kalia, V.C.; Kang, Y.C.; Lee, J.K. Synthesis of cross-linked protein-metal hybrid nanoflowers and its application in repeated batch decolorization of synthetic dyes. *J. Hazard. Mater.* **2020**, 347, 442–450.
4. Cui, J.D; Cui, L.L.; Zhang, S. P.; Zhang, Y. F.; Su, Z. G.; Ma, G. H. Hybrid magnetic cross-linked enzyme aggregates of phenyl-alanine ammonia lyase from rhodotorula glutinis. *PLoS One* **2014,** 9, 1–8.
5. de Sousa, M.; Silva, G. B.; Pessela, B. C.; Gonçalves, L. R. B. Preparation of CLEAs and magnetic CLEAs of a recombinant L-arabinose isomerase for D-tagatose synthesis. *Enzyme Microb. Technol.* **2020,** 138, 109566.
6. Vaghari, H.; Jafarizadeh-Malmiri, H.; Mohammadlou, M.; Berenjian, A.; Anarjan, N.; Jafari, N.; Nasiri, S.; Application of mag-netic nanoparticles in smart enzyme immobilization. *Biotechnol. Lett.* **2016**, 38, 223–233.
7. Otari, S. V.; Patel, S.K.S; Kim, S.Y.; Haw, J.R.; Kalia, V.C.; Kim, I.W.; Lee, J. K. Copper Ferrite Magnetic Nanoparticles for the Immobilization of Enzyme. *Indian J. Microbiol.* **2019**, **59**, 105–108.
8. Singh, R. K.; Tiwari, M. K.; Singh, R.; Lee, J. K. From protein engineering to immobilization: Promising strategies for the upgrade of industrial enzymes. *Int. J. Mol. Sci.* **2013**, 14, 1232–1277
9. Omeje, K. O.; Eze, S. O. O. Properties of partially purified peroxidase extracted from the fruit of *Solanum* spp grown in Enugu north (Variety A) and Plateau central (variety B) zones of Nigeria. *Biokemistri.* **2018**, 30, 1-12 (2018).
10. Victor, C.C.; Omeje, K.O.; Eze, S.O.O.; Ezugwu, A.L.; Chilaka, F.C.; Onwurah, I.N.E.; Ukoha, P.O. Decolorization of synthetic dyes using partially purified peroxidase from green cabbage (Brassica oleracea). *Songklanakarin J. Sci. Technol.* **2019,** 41, 783–787 (2019).
11. Chung, Y.; Tannia, D. C.; Kwon, Y. Glucose biofuel cells using bi-enzyme catalysts including glucose oxidase, horseradish pe-roxidase and terephthalaldehyde crosslinker. *Chem. Eng. J.* **2018**, 334, 1085–1092.
12. Lopes, G. R.; Pinto, D. C. G. A.; Silva, A. M. S. Horseradish peroxidase (HRP) as a tool in green chemistry. *RSC Adv.* **2014**, 4, 37244–37265.
13. Zhang, F.; Zhang, W.; Zhao, L. F.; Liu, H. Degradation of phenol with horseradish peroxidase immobilized on ZnO nanocrystals under combined irradiation of microwaves and ultrasound. *Desalin. Water Treat.* **2016**, 57, 24406–24416.
14. Balaji, V.; Arulazhagan, P.; Ebenezer, P. Enzymatic bioremediation of polyaromatic hydrocarbons by fungal consortia enriched from petroleum contaminated soil and oil seeds. *J. Environ. Biol.* **2014**, 35, 521–529.
15. Omeje, K. O.; Nnolim, N. E.; Ezema, B. O.; Ozioko, J. N.; Eze, S. O. O. Synthetic dyes decolorization potential of agroindustrial waste-derived thermo-active laccase from Aspergillus species. *Biocatal. Agric. Biotechnol.* **2020,** 29, 101800.
16. Gilman, J. C. A. *Manual of soil* fungi. 2nd ed. Iowa State College Press, Iowa, pp. 448–456 (1971).
17. Laemmli, U. K. Cleavage of structural proteins during the assembly of the head of bacteriophage T4. *Nature* **1970**, 227, 680–685.
18. Switzer, R. C.; Merril, C. R.; Shifrin, S. A highly sensitive silver stain for detecting proteins and peptides in polyacrylamide gels. *Anal. Biochem.* **1979**, 98, 231–237.
19. Eze, S. O. O. Kinetic analysis of the thermostability of peroxidase from African oil bean (Pentaclethra macrophylla Benth) seeds. *J. Biochem. Technol.* **2012**, 4, 459–463.
20. Pryce, T. M.; Palladino, S.; Kay, I. D.; Coombs, G. W. Erratum: Rapid identification of fungi by sequencing the ITS1 and ITS2 regions using an automated capillary electrophoresis system (Medical Mycology (2003) 41 (369-381)). *Med. Mycol.* **2004**, 42, 93.
21. Ranjbakhsh, E.; Bordbar, A. K.; Abbasi, M.; Khosropour, A. R.; Shams, E. Enhancement of stability and catalytic activity of immobilized lipase on silica-coated modified magnetite nanoparticles. *Chem. Eng. J.* **2012,** 179, 272–276.
22. Cruz-Izquierdo, Á.; Picó, E. A.; López, C.; Serra, J. L.; Llama, M. J. Magnetic Cross-Linked Enzyme Aggregates (mCLEAs) of Candida antarctica lipase: An efficient and stable biocatalyst for biodiesel synthesis. *PLoS One* **2014**, 9, 1–22.
23. Rehman, H. U.; Nawaz, M. A.; Aman, A.; Baloch, A. H.; Qader, S. A. U. Immobilization of pectinase from Bacillus licheniformis KIBGE-IB21 on chitosan beads for continuous degradation of pectin polymers. *Biocatal. Agric. Biotechnol.* **2014**, 3, 282–287.
24. Prajapati, J.; Dudhagara, P.; Patel, K. Production of thermal and acid-stable pectinase from Bacillus subtilis strain BK-3: Opti-mization, characterization, and application for fruit juice clarification. *Biocatal. Agric. Biotechnol.* **2021**, 35, 102063.
25. Ahmed, N. E.; El Shamy, A. R.; Awad, H. M. Optimization and immobilization of amylase produced by Aspergillus terreus using pomegranate peel waste. *Bull. Natl. Res. Cent.* **2020**, 44.
26. Wang, F.; Terry, N.; Xu, L.; Zhao, L.; Ding, Z.; Ma, H. Fungal laccase production from lignocellulosic agricultural wastes by solid-state fermentation: A review. *Microorganisms* **2019**, 7, 665.
27. Maktouf, S.; Neifar, M.; Drira, S.J.; Baklouti, S.; Fendri, M.; Châabouni, S.E. Lemon juice clarification using fungal pectinolytic enzymes coupled to membrane ultrafiltration. *Food Bioprod. Process.* **2014**, 92, 14–19.
28. da Câmara Rocha, J.; da Silva Araújo, J.; de Paiva, W.K.V.; Ribeiro, E.S.S.; de Araújo Padilha, C.E.; de Assis, C.F.; dos Santos, E.S.; de Macêdo, G.R.; de Sousa Junior, F. C. Yellow mombin pulp residue valorization for pectinases production by Aspergillus niger IOC 4003 and its application in juice clarification. *Biocatal. Agric. Biotechnol.* **2020,** 30, 101876.

29. Asgher, M.; Iqbal, H. M. N.; Irshad, M. Characterization of purified and xerogel immobilized novel lignin peroxidase produced from Trametes versicolor IBL-04 using solid state medium of corncobs. *BMC Biotechnol.* **2012**, 12, 1–8.

30. Kumar, P.; Kamle, M.; Singh, J. Biochemical characterization of Santalum album (Chandan) leaf peroxidase. *Physiol. Mol. Biol. Plants* **2011**, 17, 153–159.

31. Andriani, A.; Sukorini, A.; Perwitasari, U. Y. Enhancement of laccase production in a new isolated Trametes hirsuta LBF-AA017 by lignocellulosic materials and its application for removal of chemical dyes. *IOP Conf. Ser. Earth Environ. Sci.* **2019**, 308, 012015.

32. Khatri, B. P.; Bhattarai, T.; Shrestha, S.; Maharjan, J. Alkaline thermostable pectinase enzyme from Aspergillus niger strain MCAS2 isolated from Manaslu Conservation Area, Gorkha, Nepal. *Springerplus* **2015**, 4, 488.

33. Dange, V.; Harke, S. Production and purification of Pectinase by fungal strain in solid-state fermentation using agro-industrial bioproduct. *World J. Microbiol. Biotechnol.* **2018**, 16, 277–282.

34. Cardinali, A.; Sergio, L.; Di Venere, D.; Linsalata, V.; Fortunato, D.; Conti, A.; Lattanzio, V. Purification and characterization of a cationic peroxidase from artichoke leaves. *J. Sci. Food Agric.* **2007**, 87, 1417–1423.

35. Sandri, I. G.; Lorenzoni, C. M. T.; Fontana, R. C.; da Silveira, M. M. Use of pectinases produced by a new strain of Aspergillus niger for the enzymatic treatment of apple and blueberry juice. *LWT - Food Sci. Technol.* **2013**, 51, 469–475.

36. Osuji, A. C.; Eze, S. O. O.; Osayi, E. E.; Chilaka, F. C. Biobleaching of industrial important dyes with peroxidase partially purified from garlic. *Sci. World J.* **2014**, 183163(2014).

37. Mohamed, S. A.; Abdel-Aty, A. M.; Hamed, M. B.; El-Badry, M. O.; Fahmy, A. S. Ficus sycomorus latex: A thermostable peroxidase. *African J. Biotechnol.* **2011**, 10, 17532–17545.

38. Yihong H. Purification and partial characterization of peroxidase from lettuce stems. African J. Biotechnol. **2012**, 11, 2752–2756.

39. Mall, R.; Naik, G.; Mina, U.; Mishra, S.K. Purification and characterization of a thermostable soluble peroxidase from citrus medica leaf. Prep. Biochem. Biotechnol. **2013**, 43, 137–151.

40. Geng, Z.; Rao, K.J.; Bassi, A.S.; Gijzen, M.; Krishnamoorthy, N. Investigation of biocatalytic properties of soybean seed hull peroxidase. Catal. Today **2001**, 64, 233–238.

41. Singh, P.; Prakash, R.; Shah, K. Effect of organic solvents on peroxidases from rice and horseradish: Prospects for enzyme based applications. *Talanta* **2012**, 97, 204–210.

42. Chanwun, T.; Muhamad, N.; Chirapongsatonkul, N.; Churngchow, N. Hevea brasiliensis cell suspension peroxidase: Purification, characterization and application for dye decolorization. *AMB Express* **2013**, 3, 1–9.

43. Liu, J. Z.; Wang, T. L; Ji, L. N. Enhanced dye decolorization efficiency by citraconic anhydride-modified horseradish peroxidase. *J. Mol. Catal. B Enzym.* **2006**, 41, 81–86.

44. Sofia, P.; Asgher, M.; Shahid, M.; Randhawa, M. A. Chitosan beads immobilized Schizophyllum commune IBL-06 lignin peroxidase with novel thermo stability, catalytic and dye removal properties. *J. Anim. Plant Sci.* **2016**, 26, 1451–1463.